

Impact of the Southern Oscillation Index on Surface Water Variability in Floodplain Lake Semayang, Kalimantan, Indonesia: A Satellite Time-Series Approach

Muhammad Riza ^{a*}, Najwan Al-Ghifari ^b, Zetsaona Sihotang ^a, Nanda Khoirunisa ^a, Mislan ^c,
Idris Mandang ^a

^a Program Studi Geofisika, Fakultas Matematika dan Ilmu Pengetahuan Alam, Universitas Mulawarman, Samarinda, Indonesia

^b Program Studi Ilmu Kelautan, Fakultas Perikanan dan Ilmu Kelautan, Universitas Mulawarman, Samarinda, Indonesia

^c Program Studi Fisika, Fakultas Matematika dan Ilmu Pengetahuan Alam, Universitas Mulawarman, Samarinda, Indonesia

*Corresponding author: muhammad.riza@fmipa.unmul.ac.id

Received 26 Agustus 2025

Accepted 3 November 2025

Published 9 November 2025

DOI: 10.51264/inajl.v6i2.88

Abstract

ENSO is an important driver of hydroclimate variability in Indonesia and is strongly suspected to influence the dynamics of floodplain lakes. However, no study to date has combined the ENSO index (SOI) and satellite permanent water area time series for Lake Semayang. This study examines these linkages using 30 m resolution satellite image time series for 2000-2020. Permanent water area was obtained from JRC Global Surface Water, while SOI from NOAA. Monthly series were aligned and aggregated annually; the SOI-PWA relationship was analyzed by Pearson correlation and monthly lead-lag exploration (cross-correlation). The trend of the original annual series was tested nonparametrically with Mann-Kendall and the slope was estimated using Theil-Sen. Results showed a significant positive relationship between annual SOI and permanent water area of Semayang Lake ($r = 0.591$; $p = 0.0048$; $r^2 \approx 0.35$). Monthly explorations displayed peaks at small positive breaks, but at the annual scale the strongest relationships were contemporaneous (same year). The original annual series show no significant monotonic trend over 2000-2020 according to the Mann-Kendall test, and the Theil-Sen estimates are small with confidence intervals that include zero. This finding confirms that La Niña trending conditions are associated with permanent water area expansion, while El Niño trending conditions are associated with shrinkage, making interannual variability the main driver of lake area change. The practical implications are that SOI information can be utilized for seasonal perspectives in navigation, fisheries and flood preparedness, and integrated into regional-level water resources management and climate adaptation planning in lowland wetlands in the region.

Keywords: ENSO, Changes in water extent, SOI, Satellite imagery.

To cite this article: Riza, M., Al-Ghifari, N., Sihotang, Z., Khoirunisa, N., Mislan, & Mandang, I. (2025). Impact of the Southern Oscillation Index on Surface Water Variability in Floodplain Lake Semayang, Kalimantan, Indonesia: A Satellite Time-Series Approach. *Indonesian Journal of Limnology*, 6(2), 66–74.

This article is under license: Creative Commons Attribution 4.0 International (CC BY 4.0). <https://creativecommons.org/licenses/by/4.0/> Copyright ©2025 by author/s

1. Introduction

Floodplain lakes are important components of tropical rivers. They underpin fisheries, attenuate floods, and retain biodiversity by recording climate signals across their basins. In the Mahakam of East Kalimantan, for example, shallow lakes such as Lake Semayang are known to respond to input from precipitation and inflow. However, climate sensitivity in water levels is not well

quantified. Current satellite data records have enabled spatially consistent multi-decade monitoring at 30 m resolution, thereby providing a tractable framework to diagnose climate-hydrology coupling on water-limited continents (Pekel *et al.*, 2016; Deng *et al.*, 2024).

Similarly, an extensive literature has demonstrated that ENSO modifies hydro-climate over Indonesia. El Niño tends to suppress rainfall, while La Niña raises it and can escalate inflows to lowland floodplains. Recent studies have also emphasized the role of the IOD to modulate seasonal cycles and extremes either independently or in combination with ENSO across Indonesia and Southeast Asia. However, assessments emphasize either rainfall and extremes or lake-surface responses, with few quantifying impacts at individual floodplain lakes (Kurniadi *et al.*, 2021; Purwaningsih *et al.*, 2022; Ariska *et al.*, 2024).

Mature satellite products and cloud infrastructure provide our solution with this leap into the landscape. With input from the Landsat archive, the JRC Global Surface Water dataset locates and describes seasonal and long-term dynamics in global surface water at a confidence level to permit reliable estimation of permanent-water fraction (area) and its interannual variability. Cloud-based processing environments like Google Earth Engine ensure reproducibility and enable easy integration with climate indices (Pekel *et al.*, 2016; JRC GSW v1.4; Gorelick *et al.*, 2017).

The main purpose of this study is to measure the association between ENSO variability (characterized by the Southern Oscillation Index) and long-term variations in surface-water extent in Lake Semayang during 2000–2020. We obtain a time series of annual permanent-water area from the JRC record, analyze its year-to-year covariation with ENSO by way of correlation and trend analysis, and explore robustness across different temporal aggregations. According to the hydro-climate in Indonesia, we hypothesize that positive SOI conditions may correspond with expansion of permanent-water area, while negative ones lead to contraction (Kurniadi *et al.*, 2021; Ariska *et al.*, 2024).

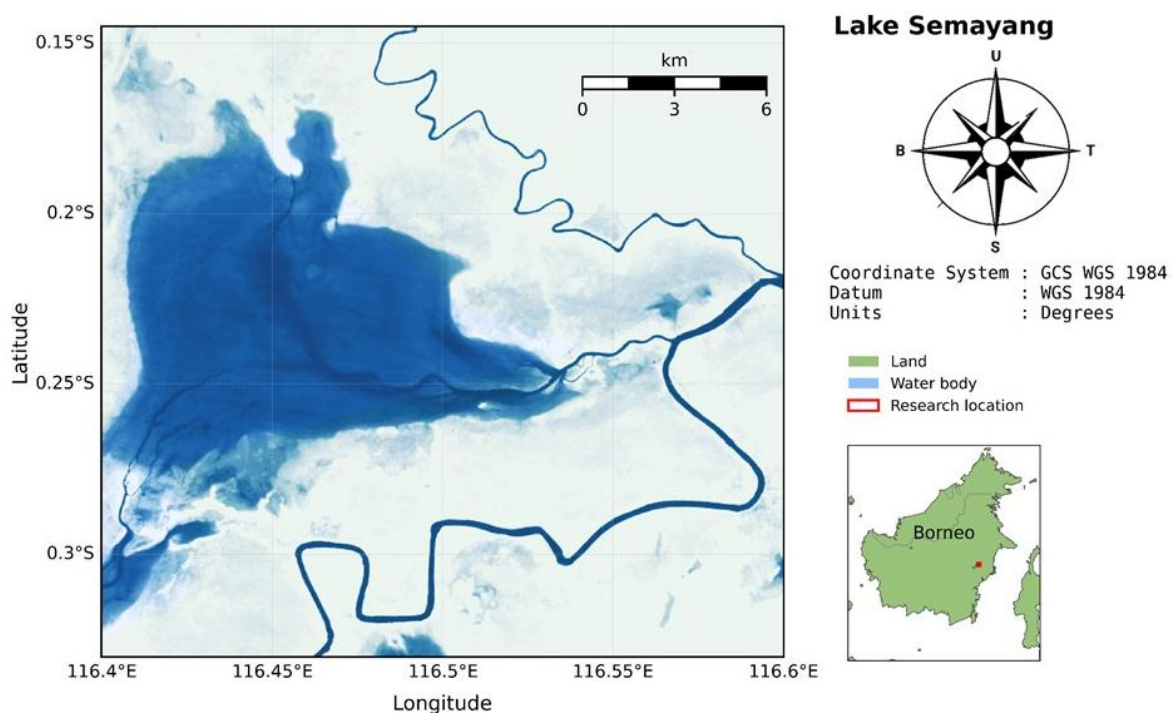


Figure 1. Research location: Lake Semayang, East Kalimantan, Indonesia

To compute PWA, aggregate climate indices, and test relationships at the interannual scale, we utilized an open and reproducible workflow. By associating satellite-based measurements of lakes with climate variability, the research helps to bridge a longstanding monitoring gap in poorly instrumented tropical floodplains. To our knowledge, this paper presents the first multi-decade satellite investigation of an ENSO signal in surface-water extent in a floodplain lake in Indonesia and the first for East Kalimantan. The workflow is applicable to other tropical lakes and wetlands

where climate-mediated hydrologic variability is of consequence for fisheries, navigation, and water-level risk management (Deng et al., 2024; Pekel et al., 2016; Gorelick et al., 2017).

2. Methods

2.1 Research Location

This research was completed at Semayang Lake (Figure 1), which is positioned between longitudes 116°40'00"E – 116°60'00"E and latitudes 0°24'00"S – 0°06'00"S. Semayang Lake is located in the eastern part of Kalimantan, bordering the Makassar Strait to the western side. Moreover, it is one of the biggest lakes in East Kalimantan.

2.2 Data

2.2.1 JRC Global Surface Water Dataset

The Joint Research Centre of the European Commission (JRC) is the internal science and knowledge service of the European Commission. The headquarters are located in Ispra, Italy, with other locations in Brussels and Geel, Belgium; Karlsruhe, Germany; Petten, Netherlands and Seville, Spain. Its main mandate is to provide scientific evidence for EU policy formulation, including remote sensing and geospatial analytics. JRC provides the Global Surface Water products via the Global Surface Water Explorer (<https://global-surface-water.appspot.com>) Engine [catalog](https://developers.google.com/earth-engine/datasets/catalog/JRC_GSW1_4_GlobalSurfaceWater) (https://developers.google.com/earth-engine/datasets/catalog/JRC_GSW1_4_GlobalSurfaceWater).

The JRC Global Surface Water Dataset was created by the Joint Research Centre (JRC) using satellite data from Landsat 5, 7, and 8, which had a spatial resolution of 30 meters. We accessed the dataset of surface water changes for Lake Semayang from the year 2000 to 2020. Included in the dataset were the following: Occurrence, Recurrence, Transitions, Seasonality, Persistence, and Extent.

2.2.2. Southern Oscillation Index (SOI)

The SOI data were obtained from the National Oceanic and Atmospheric Administration (NOAA). The Southern Oscillation Index (SOI) is the standardized index of sea-level pressure differences between Tahiti in the central Pacific and Darwin, Australia in the western Pacific. The dataset used in this research consists of monthly SOI values from 2000 to 2020. The choice of SOI is supported by recent studies showing that ENSO, as captured by SOI, strongly modulates hydroclimate variability and extremes in Indonesia and Southeast Asia, influencing rainfall, lake and catchment water availability, and monsoon behavior (Irwandi et al., 2021; Lin et al., 2024; Xu et al., 2024; Marzuki et al., 2025). The NOAA definition and data access for SOI are documented publicly.

2.3 Research Stages

This research adopted a combined approach of satellite imagery and statistical analysis. The steps included:

- 2.3.1. Analysis of climate variability and Lake Semayang's permanent water body extent,
- 2.3.2. Semayang Lake contraction and expansion dynamics,
- 2.3.3. Water class spatio-temporal analysis.

2.3.1. Water Class Spatio-Temporal Analysis

This approach demonstrates the geographic and temporal distribution of water classes within Lake Semayang. The JRC Global Surface Water dataset was the primary data source Pekel et al (2016) and was processed in Python using NumPy and pandas for data handling, GeoPandas/Shapely for vector operations, and rasterio/rioxarray for raster I/O and reprojection, with figures produced using Matplotlib (Harris et al., 2020; McKinney, 2010; Jordahl et al., 2021; Hunter, 2007). All preprocessing, analysis, and figure generation were carried out in Python 3.10 on a 64-bit Linux workstation. The workflow used the following open-source libraries:

1. Numpy 1.26 for array computation and basic numerics
2. Pandas 2.2 for tabular data handling and time-series aggregation
3. Xarray 2024.x for labeled multi-dimensional raster time series
4. Rasterio 1.3 and rioxarray 0.15 for reading and writing GeoTIFFs, coordinate reference systems, masking, and raster reprojection
5. Geopandas 0.14, shapely 2.0, and pyproj 3.6 for vector geoprocessing, geometry operations, and coordinate transforms
6. Earthengine-api 0.1xx and geemap 0.32 for accessing Google Earth Engine, exporting JRC Global Surface Water derivatives, and quick-look mapping
7. Matplotlib 3.8 for plotting maps and time-series figures
8. Scipy 1.11 and statsmodels 0.14 for correlation tests, trend estimation, and confidence intervals
9. Tqdm 4.66 for progress bars in batch processing
10. Python-dateutil 2.9 for robust date parsing and period aggregation

Processing steps included: loading lake and administrative geometries with GeoPandas; clipping and masking JRC Global Surface Water rasters to the Lake Semayang polygon with rioxarray; enforcing a consistent CRS (EPSG:4326) and pixel grid; converting permanent-water pixel counts to area in km²; aggregating to annual metrics with pandas and xarray; exporting intermediate rasters with rasterio; and computing correlations and trends with SciPy and statsmodels. Google Earth Engine collections were accessed with the official earthengine-api and scripted using geemap to export GeoTIFF and CSV outputs.

2.3.2. SOI and Permanent Water Extent Correlation Analysis

Objective. To measure the linear relationship between Southern Oscillation Index (SOI) and Permanent Water Area (PWA) of Lake Semayang in 2000-2020. PWA was calculated from JRC Global Surface Water with 30 meter resolution. Area was calculated from the number of water class pixels according to Equation (1). Changes in water area over time were analyzed against SOI to reveal trends associated with this oscillation (McBride & Nicholls, 1983).

$$\text{Water Area} = \text{Pixel Area} \times \text{Number of Water Pixels} \quad (1)$$

Data and alignment. PWA and SOI were aligned by month, then averaged by year to form n annual pairs. If a month was invalid for PWA, that month pair was excluded.

Pearson coefficient with $x_i = \text{SOI}$ and $y_i = \text{PWA}$

$$r = \frac{\sum(x_i - \bar{x}) - (y_i - \bar{y})}{\sqrt{\sum(x_i - \bar{x})^2} \sqrt{\sum(y_i - \bar{y})^2}} \quad (2)$$

Significance test. Under $H_0: \rho = 0$

$$t = r \sqrt{\frac{n-2}{1-r^2}} \quad (3)$$

With $n-2$ free degrees, two-way p values are reported. 95 percent confidence interval. Fisher transformation.

$$z = \frac{1}{2} \ln \frac{1+r}{1-r} \quad (4)$$

$$SE_z = \frac{1}{\sqrt{n-3}} \quad (5)$$

z limit $\pm 1.96 SE_z$ and then returned to r. Autocorrelation diagnostics and correction. Linearity and outliers were checked with scatterplots. For monthly data, sensitivity was tested using the effective sample size of

$$n_{eff} \approx n \frac{1 - \phi_x \phi_y}{1 + \phi_x \phi_y} \quad (6)$$

which is then used in t and interval tests. Lead lag. Cross correlations are calculated for lags of -6 to +6 months, reporting the maximum r value and its sign with multiple test adjustments.

2.3.3. Expansion and Contraction of Lake Semayang

This method calculates the changes in the surface area of Lake Semayang. Based on Equation 2, if $\Delta A > 0$, expansion occurs (the lake area increases), whereas if $\Delta A < 0$, contraction occurs (the lake area decreases).

$$\Delta A = A_{t+1} - A_t \quad (7)$$

Information:

ΔA = Change in lake area

A_{t+1} = Lake area in year t+1 (km)

A_t = Lake area in year t (km)

3. Results and Discussion

The water classification in 2011 (La Niña state) is presented in Fig. 2a, which includes categories of permanent water (blue), seasonal water (yellow), land (green), and other not-water areas (gray). The large lake in the southwest had a substantial development of permanent water (103.11 km²) while seasonal water was scattered around it, revealing variations in inundation with time. River The Pela River, a tributary or branch of Mahakam River is flowing from the southeast and supplying water to Lake Semayang.

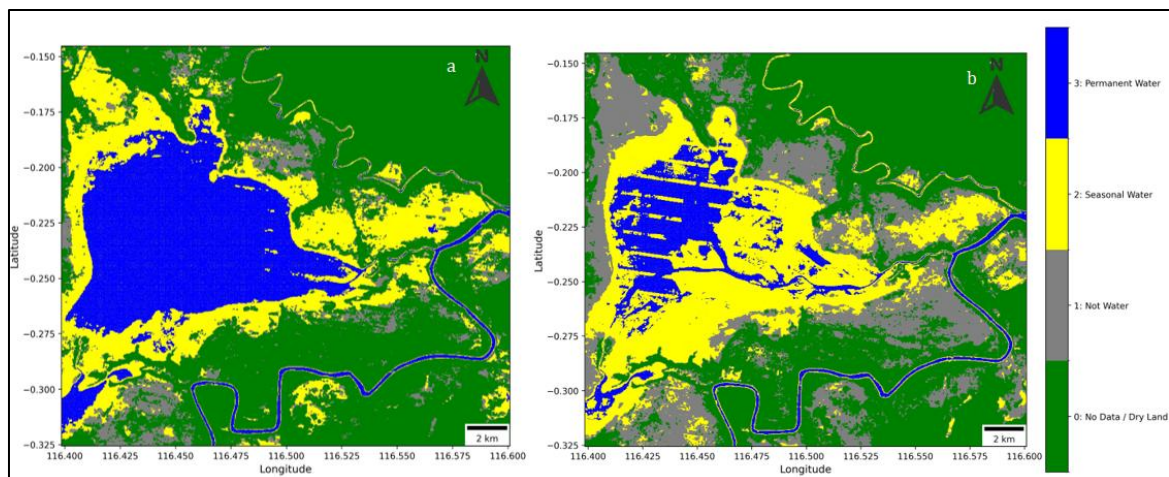


Figure 2. Water classification of Lake Semayang in (a) 2011 (La Niña) and (b) 2015 (El Niño).

By way of comparison, Figure 2b shows the water classification for 2015 under El Niño conditions. Relative to 2011, the PWA was much decreased, at merely 52.27 km² indicating drawdown of the water body, particularly to the southwest and central parts of the lake. In contrast, the seasonal water area (yellow) heaved, indicating more significant yearly changes in water depth.

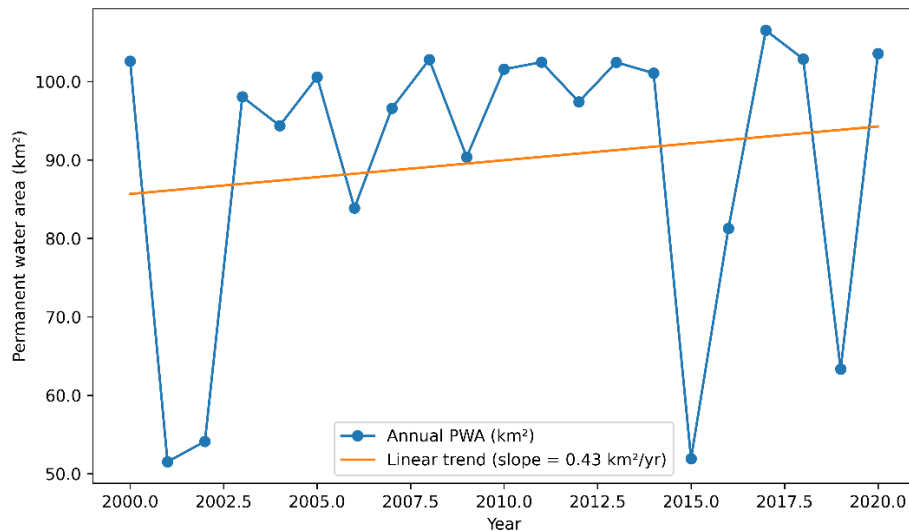


Figure 3. Annual Permanent Water Area (2000-2020)

Figure 3 presents the annual permanent water area (PWA, km²) for 2000–2020 together with a linear fit. Displaying the original series facilitates interpretation of the expansion–contraction diagnostics in Figure 4 because ΔA is the first difference of this series. Years with positive ΔA coincide with rising segments following local minima, whereas negative ΔA occur after local maxima. A Mann–Kendall test applied to the original annual series indicates no statistically significant monotonic trend ($\tau = 0.219$, $p = 0.1742$). The Theil–Sen slope is $0.323 \text{ km}^2 \text{ yr}^{-1}$ with a 95 percent confidence interval of -0.170 to $1.157 \text{ km}^2 \text{ yr}^{-1}$, which includes zero. Any apparent upward tendency in the linear fit is therefore not statistically distinguishable from no change at the 5 percent level.

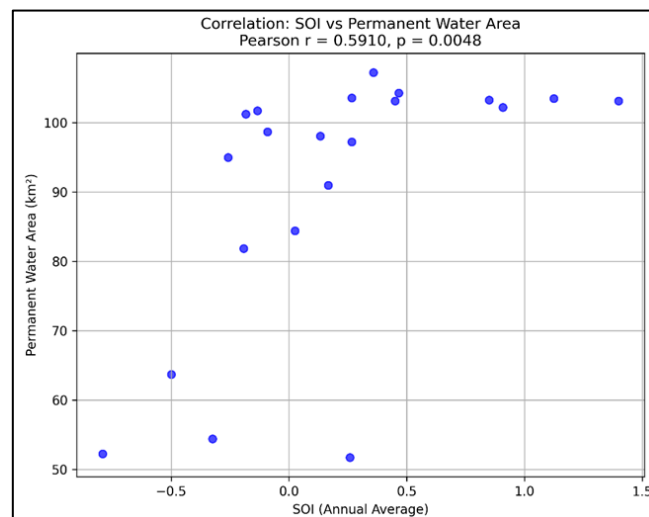


Figure 4. Correlation between SOI and permanent water area in Lake Semayang

Figure 4. Graph of annual SOI and permanent water area (km²). Using the Pearson correlation, $r = 0.5910$ with $p = 0.0048$ indicates a moderate positive association that is statistically significant at the 95 percent confidence level. Interpreting the magnitude, about 35 percent of the variance in permanent water area co-varies linearly with SOI ($r^2 \approx 0.35$). Years with higher SOI values (La Niña tendency) are associated with larger permanent water areas, whereas lower SOI values (toward El Niño events) are associated with smaller water areas. This pattern is consistent with conditions in Indonesia more broadly, where the same Köppen climate classification applies across the region and La Niña typically enhances rainfall and water supply (Aldrian & Susanto, 2003). The point cloud shows substantial dispersion, particularly at negative SOI values. Because the analysis pertains solely to Lake Semayang in Kalimantan, this dispersion reflects interannual

variability within the basin rather than differences among islands. The wider spread at negative SOI likely indicates stronger hydroclimate variability during El Niño conditions, modulated by local factors such as rainfall anomalies, inflows from the Mahakam system, and lake–floodplain connectivity, with a smaller contribution from retrieval and sampling uncertainty.

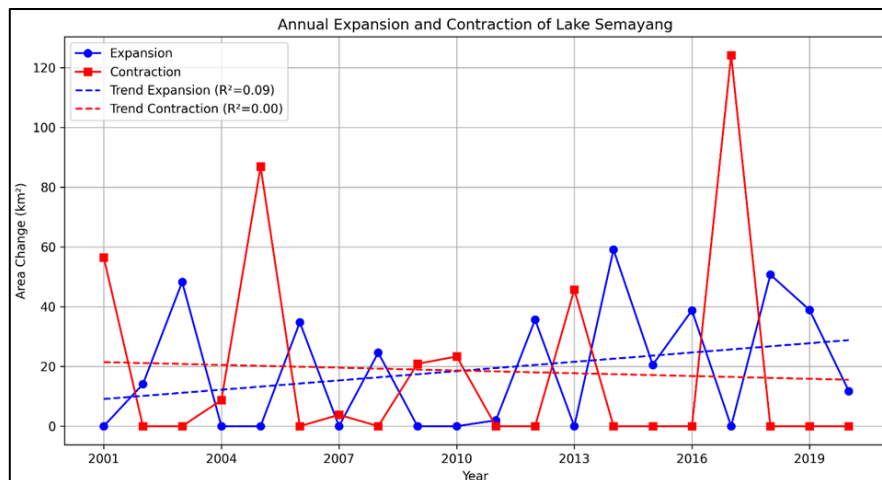


Figure 5. Expansion and contraction in Lake Semayang.

Rainfall and river inflow. Such positive relation is in line with the research hypothesis established by [Nurjaya and Setiawan \(2021\)](#) who argued that La niña is a contributor to the permanent water expansion. The water expansion of Lake Semayang is shown from 2000 to 2020 in Fig. 5, centered in annual expansions and contractions. The blue (circles) and red (squares) lines depict expansion and contraction, respectively.

2014, 2018 and 2019 had the highest expansions of 59.07 km², 50.7 km², and 38.88 km², respectively. In contrast, the largest shrinkages were reported in 2005 and 2017, when 86.85 km² and 124.12 km² disappeared, respectively. Long-term tendencies for the expansion and contraction components are illustrated with dashed linear fits. The expansion fit yields $R^2 = 0.09$ and the contraction fit $R^2 \approx 0.00$, indicating weak explanatory power of linear models for these increments. Trend inference is consequently based on nonparametric tests of the underlying PWA series. The Mann–Kendall result ($\tau = 0.219$, $p = 0.1742$) and the Theil–Sen estimate (0.323 km² yr⁻¹; 95 percent CI -0.170 to 1.157) both indicate no significant monotonic trend over 2000–2020. The expansion and contraction panels are best interpreted as interannual fluctuations around a long-term signal that is statistically stable.

Taken together, the evidence indicates that the permanent surface water area of Lake Semayang remained broadly stable during 2000–2020. Interannual variability is pronounced, but a persistent monotonic increase or decrease is not supported by the trend tests on the original series reported above.. The long-term water spread of the lake has been relatively stable, characterized by significant annual variations. The greatest expansions were in 2014, 2018 and 2019, and the most severe contractions were in 2005 and 2017. This trend is probably driven by multi-annual changes in precipitation and river influx, involving both global climatic factors and local dynamics.

These findings have significant implications for management of water resources and conservation of ecosystem surrounding Lake Semayang. Since there is a long-term expansion trend continuing, it could be considered that the lake hydrological system still has more capacity to accommodate environmental changes. Nevertheless, the high annual variability stresses the importance of more rigorous surveillance in order to predict the effects of extreme droughts that could arrive or increased flooding events due to ENSO.

The sustainability of water resource use and related aquatic ecosystems in this region should consider the climatic question to design better adaptation strategies for possible future changes. By following the principles of aquatic ecology formulated by [Wetzel \(2001\)](#), the rapid transformation of the size of a lake can influence the distribution of aquatic organisms, primary productivity and water quality requiring an assessment of hydrodynamic changes over time.

4. Conclusion

Annual SOI and permanent water area (PWA) for 2000–2020 show a positive Pearson correlation $r = 0.5910$ with $p = 0.0048$ ($n = 21$), indicating a statistically significant association; approximately 35 percent of the interannual variance in PWA co-varies linearly with SOI ($r^2 \approx 0.35$). Lead–lag exploration at the monthly scale peaks at small positive lags, but the strongest annual relationship is contemporaneous (year t). The original annual PWA series exhibits no statistically significant monotonic trend over 2000–2020 according to the Mann–Kendall test; the Theil–Sen slope estimate is small and its confidence interval includes zero.

Larger positive SOI values, reflecting La Niña conditions, are associated with larger areas of permanent water, whereas negative SOI values toward El Niño coincide with contractions of the lake's surface water. This pattern indicates that ENSO-related hydroclimate variability is a primary driver of year-to-year changes in lake extent, while a persistent long-term increase or decrease in PWA is not supported by the trend tests. From a management perspective, the emphasis should be on preparedness for interannual variability and extremes, alongside continued monitoring to detect any emerging multi-year shifts.

5. References

- Aldrian, E., & Susanto, R. D. (2003). Identification of three dominant rainfall regions within Indonesia and their relationship to sea surface temperature. *International Journal of Climatology*, 23(12), 1435-1452. <https://doi.org/10.1002/joc.950>
- Ariska, M., Irfan, M., & Iskandar, I. (2024). Spatio-temporal variations of Indonesian rainfall and their links to Indo-Pacific modes. *Atmosphere*, 15(9), 1036. <https://doi.org/10.3390/atmos15091036>
- Darmawan, S., Setiawan, B., & Nugroho, S. P. (2018). Land use change and its impact on the hydrological conditions of the Mahakam watershed. *Environmental Management and Sustainability Journal*, 7(2), 88-102.
- European Commission Joint Research Centre. (2023). Global Surface Water Mapping Layers, v1.4 (JRC/GSW1_4). Accessed March 5, 2025, from https://developers.google.com/earth-engine/datasets/catalog/JRC_GSW1_4_GlobalSurfaceWater
- GeoPandas contributors. (2020). *geopandas/geopandas: v0.8.1* (Version v0.8.1). Zenodo.
- Gillies, S., et al. (2013–2025). Rasterio: access to geospatial raster data (Documentation). Accessed March 5, 2025, from <https://rasterio.readthedocs.io/>
- Gorelick, N., Hancher, M., Dixon, M., Ilyushchenko, S., Thau, D., & Moore, R. (2017). Google Earth Engine: Planetary-scale geospatial analysis for everyone. *Remote Sensing of Environment*, 202, 18-27. <https://doi.org/10.1016/j.rse.2017.06.031>
- Harris, C. R., Millman, K. J., van der Walt, S. J., et al. (2020). Array programming with NumPy. *Nature*, 585(7825), 357-362.
- Hoyer, S., & Hamman, J. J. (2017). xarray: N-D labeled arrays and datasets in Python. *Journal of Open Research Software*, 5(1), 10.
- Hunter, J. D. (2007). Matplotlib: A 2D graphics environment. *Computing in Science & Engineering*, 9(3), 90-95.
- Kurniadi, A., Weller, E., Min, S.-K., & Seong, M.-G. (2021). Independent ENSO and IOD impacts on rainfall extremes over Indonesia. *International Journal of Climatology*, 41(6), 3640-3656. <https://doi.org/10.1002/joc.7040>
- Lin, S., Chen, C., Wang, B., Cai, W., & Lee, J.-Y. (2024). Enhanced impacts of ENSO on the Southeast Asian summer monsoon under global warming. *Geophysical Research Letters*, 51, e2023GL106437. <https://doi.org/10.1029/2023GL106437>
- Marzuki, M., Ramadhan, R., Yusnaini, H., Juneng, L., Tangang, F., Vannisa, M., Afdal., Abdillah, M. R. & Hidayat, R. (2025). Future projections of extreme precipitation over Indonesia's

- new capital under climate change scenario using CORDEX-SEA regional climate models. *Atmospheric Research*, in press. <https://doi.org/10.1016/j.atmosres.2025.108389>
- McBride, J. L., & Nicholls, N. (1983). Seasonal relationships between Australian rainfall and the Southern Oscillation. *Monthly Weather Review*, 111, 1998-2004.
- McKinney, W. (2010). Data structures for statistical computing in Python. Proceedings of the 9th Python in Science Conference, 56-61.
- NOAA Physical Sciences Laboratory. (2025). Southern Oscillation Index (SOI) monthly time series. Accessed March 5, 2025, from <https://psl.noaa.gov/data/timeseries/month/SOI/>
- Nurjaya, I. W., & Setiawan, R. Y. (2021). Impact of ENSO on the variability of permanent water area in Indonesia. *Indonesian Fisheries Research Journal*, 27(2), 103-118.
- Pekel, J-F., Cottam, A., Gorelick, N., & Belward, A. S. (2016). High-resolution mapping of global surface water and its long-term changes. *Nature*, 540, 418-422.
- Purwaningsih, A., Lubis, S. W., Hermawan, E., Fatchurohman, D., & Hadi, T. W. (2022). Moisture origin and transport for extreme precipitation over Indonesia's new capital city, Nusantara in August 2021. *Atmosphere*, 13(9), 1391. <https://doi.org/10.3390/atmos13091391>
- Python-dateutil contributors. (2024). python-dateutil (v2.9.0.post0) documentation. Accessed March 5, 2025, from <https://dateutil.readthedocs.io/>
- Rioxarray developers. (2020–2025). rioxarray documentation. Accessed March 5, 2025, from <https://corteva.github.io/rioxarray/>
- Seabold, S., & Perktold, J. (2010). Statsmodels: Econometric and statistical modeling with Python. Proceedings of the 9th Python in Science Conference, 57-61.
- Trenberth, K. E. (1997). The definition of El Niño. *Bulletin of the American Meteorological Society*, 78(12), 2771-2777.
- Virtanen, P., Gommers, R., Oliphant, T. E., et al. (2020). SciPy 1.0: Fundamental algorithms for scientific computing in Python. *Nature Methods*, 17(3), 261-272.
- Wetzel, R. G. (2001). *Limnology: Lake and River Ecosystems*. Academic Press.
- Wu, Q. (2020). geemap: A Python package for interactive mapping with Google Earth Engine. *Journal of Open Source Software*, 5(51), 2305. <https://doi.org/10.21105/joss.02305>
- Xu, L., Zhou, W., Chen, W., & Chan, J. C. L. (2022). Variations of summer extreme and total precipitation over Southeast Asia based on self-organizing maps. *Journal of Climate*, 35(19), 6291-6310. <https://doi.org/10.1175/JCLI-D-21-1020.1>